Transient absorption studies of the photochromic behavior of 3*H*-naphtho[2,1-*b*]pyran linked to a *p*-nitroaniline group

Olivier Poizat,*[a] Stéphane Aloïse,[a] Michel Sliwa,[a] Guy Buntinx,[a] Ekaterina Shilova[b] and Corinne Moustrou[b]

Received (in Montpellier, France) 16th January 2009, Accepted 27th March 2009
First published as an Advance Article on the web 8th April 2009
DOI: 10.1039/b900840c

The photophysical and photochemical behavior of a 3*H*-naphtho[2,1-*b*]pyran compound substituted at position 8 by a *p*-nitroaniline group has been investigated by transient absorption spectroscopy in the femto/picosecond and nano/microsecond time domains. Measurements were undertaken at two different pump excitation wavelengths, adjusted in resonance with the lowest energy transition S_0–S_1 (abs λ_{max} 392 nm) and with a higher energy transition S_0–S_n (abs λ_{max} 265 nm), respectively. In both cases, the results show the contribution of three transient species to the photoinduced processes: the excited S_1 and T_1 states of the initial ring-closed molecule and a long-lived colored species ascribed to a ring-opened photoproduct, attesting the presence of some photochromic activity. The S_1 and T_1 states are mainly localized on the *p*-nitroaniline substituent and do not contribute highly to the photochromic efficiency. The ring-opening photochromic process occurs essentially in $\leq$0.4 ps following excitation of the S_n state, in competition with the relaxation to the S_1 state *via* internal conversion.

Introduction

Naphthopyrans (also called benzochromenes) exhibit excellent photochromic properties, such as high colorability, rapid thermal relaxation and high resistance to fatigue, which are due to excited state electrocyclic ring opening at the pyran C–O bond.[1–4] This photoinduced reaction converts the initially colorless naphthopyran structure (ring-closed form) into a distribution of colored merocyanine isomers (ring-opened form) characterized by strongly delocalized π-electron planar configurations. These compounds are the subject of numerous investigations aimed at developing novel materials for technological applications in ophthalmic glasses, electronic display systems, optical switches and temporary or permanent memories. The inclusion of various substituents into the parent molecular skeleton is assumed to allow the wide tuning of these photochromic properties. Particular effort has been devoted to the insertion of π-electron rich substituents with the intention of extending as much as possible the π-conjugation of the ring-opened form. However, in some cases, the presence of such π-conjugated substituents may restrict the photochromic activity itself. For example, in a series of 3*H*-naphtho[2,1-*b*]pyran compounds substituted at position 8 by thiophene oligomers, the photocolorability has been observed to drop markedly or even vanish upon increasing the length of the oligothiophene chain.[5–7] From ultrafast pump–probe absorption measurements, it has been suggested that this loss of photochromic behavior is due to the appearance in these compounds of a notable π-conjugation between the naphthopyran and oligothiophenic moieties, not only in the ring-opened form, but also in the initial ring-closed form.[8] Indeed, it was assumed that as the degree of conjugation in the ring-closed form increases, the excited ππ* state involved in the photochromism decreases in energy and is less localized in the photochromic part of the molecule, engendering a barrier to the ring-opening reaction. An ideal compound should favor extended π-conjugation in the ring-opened form but no conjugation in the ring-closed form.

In this respect, we intend to explore the effect of linking an electron rich substituent to the naphthopyran structure *via* an amino junction. The amino group can adopt different conformations (pyramidal, planar) related to its propensity for *n*π conjugation. It is possible that the degree of *n*π conjugation with the naphthopyran moiety will be noticeably affected by the photochromic transformation on going from the weakly delocalized ring-closed form to the strongly delocalized ring-opened form. Important changes to the electronic conjugation through the amino junction might thus occur between the two forms. In addition, functionalization with an amino group greatly enlarges the field of potential applications, since aromatic amines are an integral part of pharmaceuticals, dyes and polymers, organic materials with important electronic properties. In the present paper, we investigate by femto/nanosecond transient absorption spectroscopy the photophysical and photochemical behavior of a 3*H*-naphtho[2,1-*b*]pyran compound substituted at position 8 by a *p*-nitroaniline group, (3,3-diphenyl-3*H*-benzo[*f*]chromen-8-yl)(4-nitrophenyl)amine (**1**) (Chart 1). The results are discussed by analogy with those obtained previously for the unsubstituted parent 3*H*-naphtho[2,1-*b*]pyran molecule, **2**.[9,10]

[a] *Laboratoire de Spectrochimie Infrarouge et Raman (UMR 8516 du CNRS), Centre d'Etudes et de Recherches Lasers et Applications (FR 2416 du CNRS), Université des Sciences et Technologies de Lille, Bât C5, 59655 Villeneuve d'Ascq Cedex, France. E-mail: olivier.poizat@univ-lille1.fr*
[b] *Centre Interdisciplinaire Nanoscience de Marseille (UPR 3118 du CNRS), Université de la Méditerranée, Faculté des Sciences de Luminy, Case 901, 13288 Marseille Cedex 9, France*

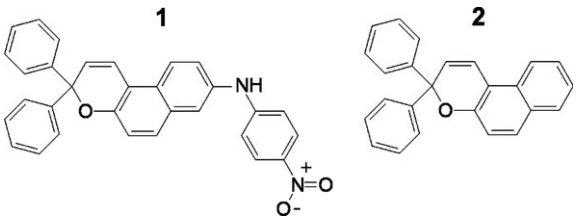

Chart 1

Results and discussion

Steady-state absorption

Fig. 1 shows the stationary absorption spectra of compounds **1** and **2**. The spectrum of **1** shows two main components, a sharp absorption band at 265 nm that corresponds roughly to the 250 nm band of **2** and a broad and structureless absorption maximized at 392 nm. The latter band might be related to the lowest energy band of **2**, which would be notably red-shifted by π-conjugation. A specific bathochromic shift of the lowest energy absorption in the presence of substituents in position 8 has in fact already been observed for various 3*H*-naphtho[2,1-*b*]pyrans, in particular, in the case of oligothiophenic substituents.[8,11] However, the 392 nm band, alternatively, might correspond to a new transition induced by the *p*-nitroaniline group, in which case it is likely to overlap the lowest energy naphthopyran transition. This point will be discussed latter. To gain a comprehensive understanding of the photophysical properties of **1**, transient absorption measurements were carried out at two pump excitation wavelengths set in resonance with the 265 and 392 nm transitions, respectively.

Femto/picosecond dynamics

We consider first the very short-time photoinduced spectral evolution occurring on the sub-nanosecond timescale. Fig. 2 and Fig. 3 show femto/picosecond transient absorption spectra obtained for compound **1** in acetonitrile at different pump–probe time delays following excitation at 383 and 266 nm, respectively. Although the spectral domain probed with the 383 nm pump configuration is much reduced compared to that probed with the 266 nm pump configuration (owing to the different optical filters used for rejecting the pump light), the same 300–700 nm spectral scaling is used in Fig. 2 and Fig. 3 to facilitate comparison. Upon excitation at 383 nm (Fig. 2), that is, within the lowest energy absorption band of **1**, the initial transient absorption spectrum is characterized by a negative bleach component peaking at 410 nm, consistent with the steady-state spectrum of **1** (Fig. 1), and a broad transient absorption band peaking at 470–500 nm and extending beyond 700 nm. The intensities of both the bleach and absorption bands, as measured by the band area, are at their maximum at the shortest time delay (0.5 ps) and decay with practically unique exponential kinetics, with a time constant of 1.5 ± 0.2 ps. The short-time transient absorption spectrum thus most likely characterizes the S_1 state of **1**, which is directly excited at 383 nm. The almost complete decay (~95%) of the bleach component concomitant with the S_1 state absorption decay indicates that the S_1 state relaxes mainly *via* fast internal conversion (IC) to the initial ground state. The decay of the S_1 state absorption band is accompanied by a *ca.* 30 nm continuous blue-shift of its maximum, which is ascribable to some vibrational/conformational/solvation relaxation process. The time dependence of the position of the absorption maximum can be satisfactorily fitted with a mean 0.7 ps exponential kinetics. At the end of the decay kinetics of S_1, a weak residual bleach signal (~5%) and a very small absorption band at *ca.* 490 nm are still present and keep a nearly constant intensity over the 30 ps–3 ns time

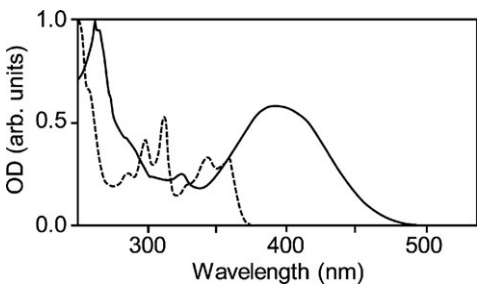

Fig. 1 Normalized absorption spectra of **1** (solid line) and **2** (dashed line) in acetonitrile.

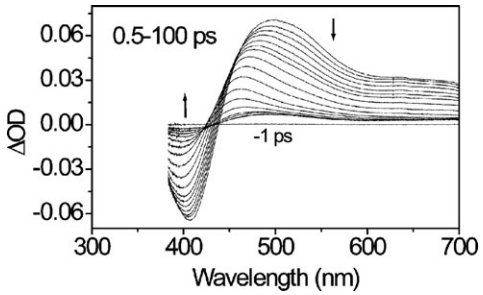

Fig. 2 Transient absorption spectra of **1** in acetonitrile at different time delays (0.5, 0.6, 0.7, 0.8, 0.9, 1.0, 1.3, 1.6, 2.0, 3.0, 5.0, 10, 20, 30, 50 and 100 ps) after excitation at 383 nm. Vertical arrows indicate the signal evolution.

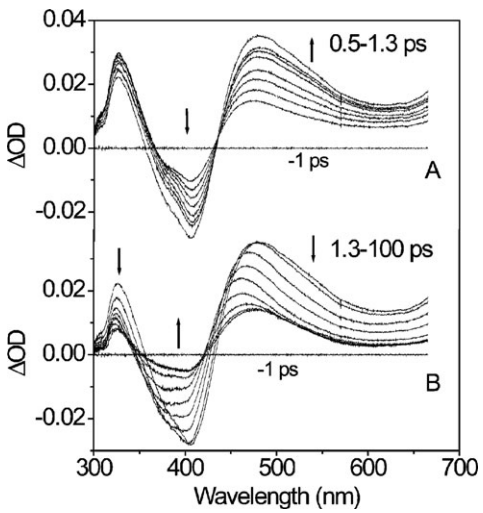

Fig. 3 Transient absorption spectra of **1** in acetonitrile at different time delays after excitation at 266 nm: (A) 0.5, 0.6, 0.7, 0.8, 0.9, 1.0, 1.1 and 1.3 ps; (B) 1.3, 1.8, 2.0, 2.4, 3.0, 5.0, 10, 20 and 100 ps. Vertical arrows indicate the signal evolution.

domain. This indicates that, despite the fast deactivation of S_1 by IC to S_0, about 5% of the S_1 population leads to the formation of photoproducts.

Upon excitation at 266 nm (Fig. 3), which corresponds to a higher energy $S_0 \rightarrow S_n$ transition of **1**, the short-time spectra show the same 470–500 nm transient absorption and 410 nm bleach components as upon 383 nm excitation, plus a second transient absorption at 325 nm, detected due to the larger spectral window available at 266 nm. In contrast to the dynamics observed with the 383 nm pump, these components increase in intensity up to 1.3 ps (part A in Fig. 3, time constant $\leq$0.4 ps) before decaying with 1.7 $\pm$ 0.4 ps kinetics (part B in Fig. 3). According to the similarity of the spectral features and decay kinetics at both pump wavelengths, this spectrum is readily assigned to the S_1 state of **1**. The observed sub-picosecond rise kinetics are likely to characterize the dynamics of the population of the S_1 state *via* IC from the initially pumped S_n state, which will be discussed later. The bleach component disappears almost entirely ($\sim$85%) during the decay of the S_1 absorption, which implies that, as upon 383 nm excitation, the main deactivation route of the S_1 state is by IC to the ground state. However, the intensity of the residual absorption spectrum at 100 ps relative to the initial intensity of the precursor S_1 state spectrum is significantly larger than upon excitation at 383 nm. Again, this residual spectrum maintains a nearly constant intensity from 30 ps to 3 ns. Therefore, although IC to the ground state remains the dominant deactivation route of the S_1 state, the yield of formation of photoproducts appears higher with 266 nm excitation.

Nano/microsecond dynamics

Fig. 4 and Fig. 5 show nano/microsecond laser flash photolysis spectra of **1** recorded after 355 and 266 nm excitation, respectively, in de-aerated acetonitrile. The same 300–700 nm spectral scaling is used for all of Fig. 2–5. The spectrum observed with a delay of 140 ns after the 266 nm excitation of **1** in acetonitrile (Fig. 5) resembles manifestly the one measured after 30 ps in the femto/picosecond experiment (Fig. 3), with absorption components at 490 and 330 nm, and a weak bleach signal in the 400 nm region. This spectrum evolves slightly within 1 μs then keeps a constant shape and intensity over the 200 μs range of our measurement. Similar spectra are recorded upon excitation at 355 nm (Fig. 4), but

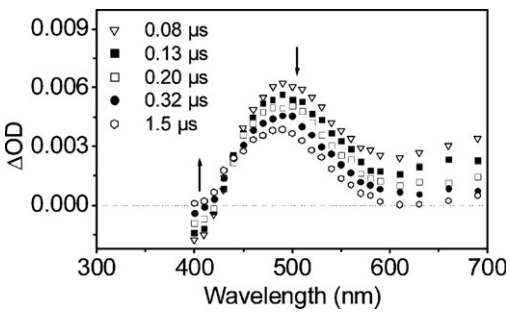

Fig. 4 Laser flash photolysis spectra obtained at different time delays from 0.08 to 1.5 μs after the 355 nm excitation of a de-aerated solution of **1** in acetonitrile. Vertical arrows indicate the signal evolution.

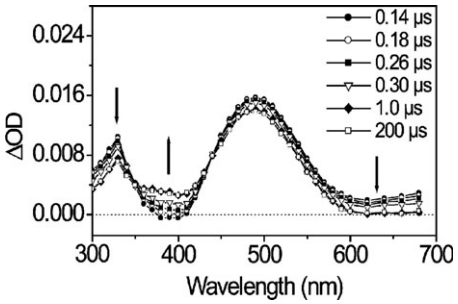

Fig. 5 Laser flash photolysis spectra obtained at different time delays from 0.14 to 200 μs after the 266 nm excitation of a de-aerated solution of **1** in acetonitrile. Vertical arrows indicate the signal evolution.

their intensity is much less than in the 266 nm experiment. This low intensity is consistent with the notable intensity reduction observed above for the 30 ps spectrum upon changing the excitation wavelength from 266 nm (Fig. 3) to 383 nm (Fig. 2).

The 1 μs spectral evolution seen in Fig. 5 is characterized by a small decay in intensity above 500 nm and below 330 nm, and an increase in the bleach region. As can be seen in Fig. 6, the associated kinetics, characterized by a time constant of 300 ns in de-aerated acetonitrile, is drastically shortened in the presence of air. In contrast, neither the intensity nor the lifetime of the residual spectrum observed at time delays longer than 1 μs are affected by the presence of air. Therefore, besides the ground state bleach, the spectra measured in the nano/microsecond time range are due to the superposition of two contributions: a minor component due to an air-sensitive species of 300 ns lifetime and a main component due to a long-lived and air-insensitive species (its lifetime was nevertheless too short to allow its detection by steady-state absorption). Considering that this second component keeps a constant intensity at all times, subtracting the 1 μs spectrum from all the spectra in the 0–1 μs time range in Fig. 5 leads to the spectral evolution displayed in Fig. 7, that thus characterizes the decay of the air-sensitive species and the associated ground state bleach recovery. The common kinetics measured at all wavelengths, and the clear isosbestic points observed at 345 and 445 nm between the bleach recovery and the transient absorption decay, confirm clearly that the relaxation of the air-sensitive transient species leads back to the initial ground state of **1**.

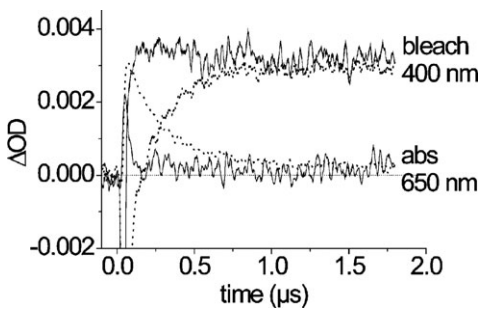

Fig. 6 Normalized kinetic traces measured at 400 nm (bleach recovery) and 650 nm (absorption decay) for a de-aerated solution of **1** in acetonitrile (dotted line) and the same aerated solution after 266 nm excitation (solid line).

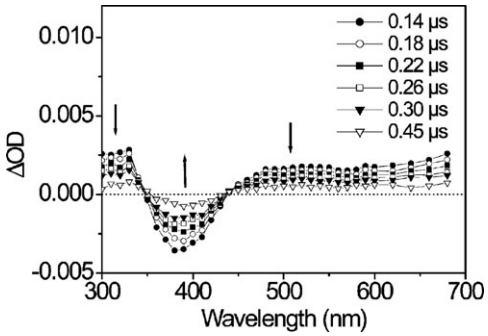

Fig. 7 Transient spectra processed by subtracting the 1 μs spectrum from the 0.14–0.45 μs spectra in Fig. 5. Vertical arrows indicate the signal evolution.

According to the above results, we assign unambiguously the air-sensitive transient species to the lowest excited triplet state, T_1, of **1**, formed from the S_1 state *via* intersystem crossing (ISC). By analogy with previous results concerning the photophysical and photochemical characteristics of the 3*H*-naphtho[2,1-*b*]pyran family of compounds, we ascribe with quite good confidence the long-lived, air-insensitive species absorbing at 490 nm to the ring-opened form of **1**, resulting from the photochromic reaction. Comparing the nano/microsecond spectra recorded upon 355 and 266 nm pump excitation (Fig. 4 and Fig. 5, respectively) shows that the much lower intensities of the spectra pumped at 355 nm are due to a much weaker contribution of the long-lived residual component characterizing the ring-opened photoproduct.

The photophysical and photochemical behavior of 1

The characterization of the ring-opened form of photoproduct **1** reveals the photochromic character of this molecule. An important question concerns the origin of this ring-opened species, *i.e.*, the nature of the excited state in which the photochromic process occurs. In this regard, a joint analysis of the complementary results obtained by steady-state absorption and by transient absorption in the femto/picosecond and nano/microsecond time domains, on one hand, and upon light excitation at 266 nm and above 350 nm, on the other hand, allows us to propose a plausible picture of the photophysical and photochemical behavior of **1**.

It is clear that excitation at 266 nm as well as above 350 nm results in the formation of the same very short-lived lowest excited singlet state, S_1 ($t_{1/2} \sim 1.5$ ps), which deactivates mainly by IC to the S_0 state . The population of S_1 is achieved directly at $\lambda_{pump} > 350$ nm or *via* a higher excited S_n state at $\lambda_{pump} = 266$ nm. As discussed above, the 265 nm $S_0 \rightarrow S_n$ absorption of **1** is likely to be related to a similar absorption of the unsubstituted parent compound, **2**, at 250 nm and thus characterizes the naphthopyran chromophore. In contrast, the lowest energy $S_0 \rightarrow S_1$ absorption at 392 nm, red-shifted in **1** relative to **2**, is likely to involve the *p*-nitroaniline substituent. Our observation that the $S_n \rightarrow S_1$ IC process, following excitation of S_n at 266 nm, is characterized by an increase of the bleach signal at the position of the $S_0 \rightarrow S_1$ absorption (400 nm region), as well as of the S_1 state transient absorption (Fig. 3A), suggests that the chromophores of the $S_0 \rightarrow S_1$ and $S_0 \rightarrow S_n$ transitions are practically independent and decoupled from each other. In other words, the $S_0 \rightarrow S_1$ transition is mostly localized in the *p*-nitroaniline substituent and the $S_0 \rightarrow S_n$ transition principally affects the naphthopyran moiety. In this respect, the rise of the bleach component observed at the position of the $S_0 \rightarrow S_1$ absorption during the IC from S_n to S_1 can be considered as an indicator that this IC process corresponds to an intramolecular energy transfer from the naphthopyran group to the *p*-nitroaniline substituent (time constant ≤ 0.4 ps). Such a rise of the bleach intensity would not be observed if the S_1 absorption at 392 nm was due to a naphthopyran transition shifted due to electronic conjugation by the *p*-nitroaniline substituent. Note that this assignment does not wipe out the presence of the lowest energy transition of the naphthopyran moiety that is expected to arise, as in **2**, in the 300–380 nm region, slightly above the $S_0 \rightarrow S_1$ transition and considered in the following as an $S_0 \rightarrow S_2$ transition.

The assumption that the S_1 state of **1** is essentially localized on the *p*-nitroaniline group is consistent with the observation of substantial analogies between the S_1 states of *p*-nitroaniline (PNA)[12] and *N*,*N*-dimethyl-*p*-nitroaniline (DPNA),[13] concerning their dynamics and spectral properties. Indeed, the $S_0 \rightarrow S_1$ absorption band of **1** is quite comparable in shape and position to the strong $S_0 \rightarrow S_1$ charge transfer band observed for PNA (λ_{max} 365 nm)[12] and DPNA (λ_{max} 385 nm)[13] in acetonitrile. The short-lived character of S_1 (about 1.5 ps) is also in agreement with the ultrafast S_1 decay kinetics reported for PNA (0.30 ps) and DPNA (0.63 ps) in acetonitrile.[14] In these two molecules, it has been established that the S_1 state is characterized by intramolecular charge transfer from the amino group to the nitro group, which undergoes a twisting motion. Ultrafast IC to the ground state occurs through a conical intersection present along the NO_2 twisting coordinate.[12,14] IC is in competition with fast ISC to the T_1 state ($\Phi_{ISC} = 0.03$ and 0.4 for PNA in water and dioxane, respectively), favored in non-polar solvents by substantial mixing of the S_1 and T_1 states, which are nearly degenerate.[15] Therefore, we suggest that the nature and dynamics of the S_1 and T_1 states of **1** are reminiscent of the corresponding states in PNA and DPNA, which explains satisfactorily the minor photochromic efficiency observed in S_1 relative to S_n.

According to the analogy of the 30 and 100 ns spectra, a mixture of the T_1 state and the ring-opened form is found to already be present at the end of the S_1 state decay kinetics, but with relative contributions strongly dependant on the pump wavelength. Upon excitation at $\lambda_{pump} > 350$ nm, the S_1 state is populated directly and relaxes at 95% by IC to the S_0 state. The nano/microsecond data obtained at 355 nm reveal that the remaining 5% of S_1 state molecules undergo, at least largely, ISC to the T_1 state. A weak absorption component due to the ring-opened colored form is nevertheless perceptible (1.5 μs spectrum in Fig. 4). This can possibly be explained by a minor absorption of the S_2 state at 355 nm localized on the naphthopyran group and, as discussed above, lying presumably at an energy close to the S_1 state. It might also be due to a low efficiency ring-opening process arising directly in the *p*-nitroaniline-localized S_1 state due to a weak coupling with the naphthopyran-localized S_2 state. It must be remarked that in the femto/picosecond measurements made at 383 nm,

because of the probably weaker resonance of the $S_0 \rightarrow S_2$ transition than at 355 nm, it is not possible to determine whether the residual spectrum observed after the decay of the S_1 state (100 ps spectrum in Fig. 2) contains a contribution from the ring-opened species, in addition to the T_1 state, or is due only to T_1. In any case, excitation at $\lambda_{pump} > 350$ nm leads to very little ring-opened photoproduct ($\ll 5\%$).

Upon 266 nm excitation, the population of the S_1 state is achieved indirectly *via* a higher excited S_n state within 0.4 ps and relaxes mostly by IC to S_0. The residual spectrum observed after the decay of S_1 is notably more intense, relative to the initial intensity of the S_1 spectrum, than that for the excitation at >350 nm and is mostly due to the ring-opened photoproduct. If at both excitation wavelengths the ISC and ring-opening processes were taking place in the same precursor excited S_1 state, their relative yield should be independent of the pump wavelength. We conclude that most of the ring-opened species produced at 266 nm do not arise from the S_1 state. Two possible mechanisms can be envisaged. In the first hypothesis, the ring-opening reaction can be imagined as arising mainly from the upper S_n state in ≤ 0.4 ps, in competition with the deactivation of S_n to S_1 by IC. An alternative mechanism is to consider that the deactivation of S_n to S_1 occurs *via* the naphthopyran-localized S_2 state, and that the ring-opening reaction occurs in S_2 before relaxation to S_1. In this second hypothesis, the stronger reaction efficiency observed upon excitation at 266 nm than at >350 nm can be explained by the more efficient population of S_2 *via* IC from S_n than by direct excitation at $\lambda_{pump} > 350$ nm and/or by a faster ring-opening reaction in S_2 due to a larger excess of vibrational energy contained in the S_2 state produced by relaxation from S_n. Scheme 1 shows a tentative overall description of the photophysical and photochemical behavior of **1** that summarizes these comments. This description remains rather approximate and qualitative due to the complexity of such a molecular structure, where two different chromophores are present and can be simultaneously excited with relative yields depending on the excitation wavelength.

It can be observed in Fig. 2 and Fig. 3 that a small spectral evolution is observed in the 10–30 ps timescale, *i.e.*, after the complete deactivation of S_1. This evolution takes place in the 350–480 nm region and is mainly characterized by a red-shift of the absorption maximum from 465 to 490 nm, associated with some decay of the bleach signal. This might reflect the presence of some vibrational relaxation of the hot ground state molecules produced from the fast and efficient $S_1 \rightarrow S_0$ IC deactivation process. In fact, with hot molecules, having broader absorptions than cold molecules, their formation is expected to be characterized by an incomplete bleach recovery and the presence of positive absorption wings at the edges of the bleach signal. In this case, the absorption band narrowing effect accompanying the cooling dynamics is assumed to progressively decrease the absorption wings and fill up the bleach signal, which corresponds quite well with the observed 10–30 ps spectral evolution seen in Fig. 2 and Fig. 3. In this hypothesis, the difference between the 10 and 30 ps spectra thus accounts for the presence in the former of a contribution from hot ground state molecules, in addition to the T_1 state and ring-opened form. An alternative plausible interpretation of the 10–30 ps spectral evolution could be the existence of some conformational evolution of the ring-opened form. In fact, it is known for parent compound **1** and several of its substituted derivatives that the ring-opening reaction leads first to a *cis* ring-opened isomer that evolves towards a final thermal equilibrium involving a mixture of *trans* isomers, with complex dynamics characterized by at least two time constants in the 1–3 and 10–20 ps time domains, respectively.[8–11]

A final remark concerns the position of the ring-opened form absorption band of **1**, peaking at 490 nm. This absorption is strongly red-shifted relative to the 425 nm absorption maximum of the corresponding ring-opened form of parent unsubstituted molecule **2**.[9,10] It is also somewhat shifted compared to compounds substituted at position 8 by electronically-conjugated substituents, such as phenylethynyl (λ_{max} 460 nm) or dithienylethynyl (λ_{max} 485 nm) groups.[8,11] This red-shift reveals the existence of an important π-conjugation in the ring-opened form between the naphthopyran and *p*-nitroaniline moieties through the amino group, although, as shown above, these two moieties are practically electronically uncoupled in the ring-closed form. In this respect, **1** clearly differs from its related compounds substituted at position 8 by thiophene oligomers, for which the presence of electronic coupling in the ring-closed form is also a limiting factor in the ring-opening photoreaction yield.

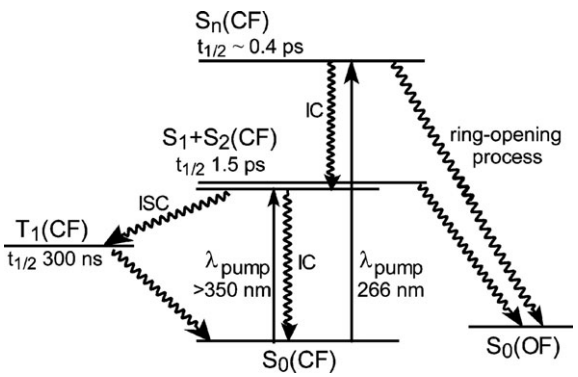

Scheme 1 A schematic representation of non-radiative relaxation processes after the light excitation of **1** (CF, OF: ring-closed, ring-opened forms; ISC intersystem crossing; IC internal conversion).

Conclusion

A comparison of pump–probe transient absorption data obtained for a 3*H*-naphtho[2,1-*b*]pyran compound substituted at position 8 by a *p*-nitroaniline group (compound **1**) in the femto/picosecond and nano/microsecond time domains, and with two pump excitations at 266 nm and above 350 nm, allowed us to propose a plausible picture of its photophysical and photochemical behavior. Measurements were undertaken at two different pump excitations adjusted to be in resonance with the lowest energy transition (S_0–S_1, abs λ_{max} 392 nm) and with a higher energy transition (S_0–S_n, λ_{max} 265 nm), respectively. The contribution of three transient species to the photoinduced processes was in evidence: the excited S_1 and T_1 states of the initial ring-closed molecule and a long-lived

colored species ascribed to a ring-opened photoproduct, attesting the presence of some photochromic activity. The S_1 and T_1 states are mainly localized on the *p*-nitroaniline substituent and do not contribute significantly to the photochromic activity of the molecule. The ring-opening photochromic process occurs essentially in $\leq$0.4 ps *via* excitation of the higher-lying S_n state, which is mostly localized on the naphthopyran moiety, in competition with relaxation to the S_1 state *via* IC. IC from S_n to S_1 corresponds to an intramolecular energy transfer from the naphthopyran group to the *p*-nitroaniline substituent. Whereas the naphthopyran and *p*-nitroaniline moieties are electronically de-coupled in the ring-closed form, a 65 nm red-shift of the ring-opened form absorption, relative to its position in the unsubstituted naphthopyran molecule, reveals a notable electronic π-delocalization over the entire molecule in the ring-opened form. This type of amino-substituted naphthopyran compound might thus be attractive in view of applications in optoelectronic devices, such as organic photoswitches of conductivity, or in the utilization of its non-linear optical properties.

Experimental

The synthesis of (3,3-diphenyl-3*H*-benzo[*f*]chromen-8-yl)-(4-nitrophenyl)amine (**1**) has already been reported,[16,17] and was performed by using a convenient approach for introducing amino groups into chromene molecules based on the palladium-catalyzed amination method (Buchwald–Hartwig C–N coupling). ^{1}H and ^{13}C NMR characterization of **1**, as well as the determination of its molecular structure by X-ray crystallography, has also previously been reported.[17] The acetonitrile solvent (Aldrich, spectrophotometric grade) was used as supplied, without further purification.

The femtosecond transient absorption setup has already been described.[18] Briefly, it involves a 1 kHz Ti-sapphire laser system based on a Coherent (MIRA 900D) oscillator and a BM Industries (ALPHA 1000) regenerative amplifier. Pump excitation at 383 and 266 nm ($<$150 fs, 3–15 μJ per pulse, 0.3–1.5 mJ cm^{-2}) was obtained by frequency doubling the Ti-sapphire fundamental, tuned at 766 nm, or frequency tripling the fundamental, tuned at 800 nm, respectively (0.3 mm BBO crystals). A white light continuum probe pulse was generated by focusing the 766 or 800 nm beam at a 1 mm CaF_2 plate. The pump–probe polarization configuration was set at the magic angle (54.7°). The probe pulse was delayed relative to the pump pulse by using an optical delay line (Microcontrol Model MT160-250PP driven by an ITL09 controller, precision 1 μm). The overall time resolution (FWHM of the pump–probe intensity cross-correlation) was estimated to be about 300 fs from the two-photon (pump + probe) absorption signal in pure hexane. The time dispersion of the continuum light over the 300–700 nm region of analysis was about 0.8 ps. The transmitted light was sent to the entrance slit of a 230 mm focal length stigmatic spectrograph equipped with 150 groove mm^{-1} grating and analyzed by a charge-coupled device (CCD) optical multi-channel analyzer (Princeton Instrument LN/CCD-1340/400-EB detector + ST-138 controller). Sample solutions (OD $\sim$ 1.0 and 0.5 at 266 and 383 nm, respectively) were circulated in a flow cell equipped with 0.2 mm thick CaF_2 windows and characterized by a 2 mm optical path length. Data were accumulated over 3 min ($<$180 000 pump–probe sequences).

Nano/microsecond transient absorption experiments were performed using a laser flash photolysis apparatus. Excitation pulses at 355 and 266 nm (7–8 ns, 1 mJ) were provided by a 20 Hz Nd:YAG laser (DIVA II, Thales laser). The probe light was provided by a Xe lamp (XBO 150 W/CR OFR, Osram). Samples were contained in a quartz cell (10 × 10 mm section) at a concentration adjusted to give an OD value of $\sim$1.0 at the pump excitation wavelength. All solutions were de-aerated by bubbling with N_2, apart from those used for measuring the effect of quenching by O_2. The transmitted light was analyzed by a spectrometer equipped with a photomultiplier (R1477-06, Hamamatsu) coupled to a digital oscilloscope (TDS 540, Tektronix).

Acknowledgements

The authors thank the Groupement de Recherche GDRI 93 from CNRS and the Centre d'études et de Recherches Lasers et Applications (CERLA) for their help in the development of this work. CERLA is supported by the Ministère chargé de la Recherche, Région Nord/Pas de Calais, and the Fonds Europe en de Développement Economique des Régions.

References

1 R. C. Bertelson, in *Techniques of Chemistry*, ed. G. H. Brown, Wiley, New York, 1971, vol. 3, pp. 45.
2 J. R. Guglielmetti, in *Photochromism: Molecules and Systems*, ed. H. Dürr and H. Bouas-Laurent, Elsevier, Amsterdam, 1990, pp. 314.
3 B. Van Gemert, in *Organic Photochromic and Thermodynamic Compounds*, ed. J. C. Crano and J. R. Guglielmetti, Plenum Press, New York, 1999, vol. 1, pp. 111.
4 R. S. Becker and J. Michl, *J. Am. Chem. Soc.*, 1966, **88**, 5931.
5 M. Frigoli, C. Moustrou, A. Samat and R. Guglielmetti, *Helv. Chim. Acta*, 2000, **83**, 3043.
6 M. Frigoli, C. Moustrou, A. Samat, R. Guglielmetti, R. Dubest and J. Aubard, *Mol. Cryst. Liq. Cryst.*, 2000, **344**, 139.
7 S. Coen, C. Moustrou, M. Frigoli, M. Julliard, A. Samat and R. Guglielmetti, *J. Photochem. Photobiol., A*, 2001, **139**, 1.
8 B. Moine, J. Rehault, S. Aloïse, J.-C. Micheau, C. Moustrou, A. Samat, O. Poizat and G. Buntinx, *J. Phys. Chem. A*, 2008, **112**, 4719.
9 J. Aubard, F. Maurel, G. Buntinx, O. Poizat, G. Levi, A. Samat and R. Guglielmetti, *Mol. Cryst. Liq. Cryst.*, 2000, **345**, 215.
10 P. L. Gentili, E. Danilov, F. Ortica, M. A. J. Rodgers and G. Favaro, *Photochem. Photobiol. Sci.*, 2004, **3**, 886.
11 B. Moine, G. Buntinx, O. Poizat, J. Rehault, C. Moustrou and A. Samat, *J. Phys. Org. Chem.*, 2007, **20**, 936.
12 V. M. Farztdonov, R. Schanz, S. A. Kovalenko and N. P. Ernsting, *J. Phys. Chem. A*, 2000, **104**, 11486.
13 Y. Kimura, T. Hamamoto and M. Terazima, *J. Phys. Chem. A*, 2007, **111**, 7081.
14 S. A. Kovalenko, R. Schanz, H. Hennig and N. P. Ernsting, *J. Chem. Phys.*, 2001, **115**, 3256.
15 C. L. Thomsen, J. Thogersen and S. R. Keiding, *J. Phys. Chem. A*, 1998, **102**, 1062.
16 E. A. Shilova, C. Moustrou and A. Samat, *Tetrahedron Lett.*, 2005, **46**, 8857.
17 E. A. Shilova, V. P. Perevalov, A. Samat and C. Moustrou, *Tetrahedron Lett.*, 2007, **48**, 4127.
18 G. Buntinx, R. Naskrecki and O. Poizat, *J. Phys. Chem.*, 1996, **100**, 19380.

